

**Reversible assembly of gold nanoparticles confined in an optical microcage**

Hiroyuki Yoshikawa,\* Togo Matsui, and Hiroshi Masuhara

*Department of Applied Physics and Frontier Research Center, Osaka University, 2-1 Yamada-oka, Suita, Osaka 565-0871, Japan*

(Received 28 July 2004; published 13 December 2004)

As optical trapping by a focused laser beam is applied for nanoparticles, multiple particles are grasped in the focal spot and make an assembly. Gold nanoparticles confined in such a submicrometer optical cage show a characteristic extinction spectrum depending on laser power. The spectral change can be induced reversibly and repeatedly by tuning the laser power, demonstrating that the assembly of gold nanoparticles can be controlled by the gradient force. This is attributed to the soft confinement of nanoparticles dressed in electrostatic potential barriers.

DOI: 10.1103/PhysRevE.70.061406

PACS number(s): 61.43.Hv, 87.80.Cc, 61.46.+w, 87.64.Ni

**I. INTRODUCTION**

Colloidal particles are expected to be characteristic materials for electrical, optical, chemical, and biological applications. In addition to individual nanoparticles, assemblies of nanoparticles are interesting research targets due to their collective properties. Weak interparticle interactions, which are comparable with the thermal energy, give flexibility for colloidal assemblies, so that their conformations are easily changed by temperature, concentration,  $pH$ , and so forth. On the other hand, their flexible but fragile assembling structures and accompanying properties make their micro- and nanofabrication difficult. Many researchers have attempted to fabricate colloidal assemblies by various approaches. Although self-assembly is one of the most promising techniques to fabricate micro- or nanostructures of colloidal particles, arbitrary structures cannot be obtained by this approach. Therefore other methods to fabricate a controlled colloidal assembly with submicrometer dimensions are desired. Considering this background, we have proposed optical trapping of various colloidal materials [1–4].

In the past decade, optical trapping by a focused laser beam has been used for manipulation of individual microparticles in solution. Corresponding to developments in nanoscience and nanotechnology, this technique has recently been developed and extended to nanoparticles. The focused laser beam makes a strong gradient of the electromagnetic field. A nanoparticle, which can be regarded as an electric dipole, experiences an attractive force into the center of the laser focus where the intensity of the electromagnetic field is at a maximum (i.e., the potential energy is at a minimum). This force is called the optical gradient force [5,6]. It is worth noting that the potential energy produced by the gradient force is strong enough to confine nanoparticles for a while in the focal spot, but nanoparticles confined in the focal spot can rearrange their positions to form the most stable assembly. Therefore we expect that micro- or submicrocolloidal assemblies with ordered structures on the nanometer scale

can be fabricated by optical trapping. There has so far been some work studying conformational change of colloidal assemblies by means of optical trapping. Jose and Bagchi investigated the dynamics and structure of molecules under optical trapping by using a Brownian dynamics simulation [7], and reported that optical trapping enhances formation of molecular clusters. Korda and Grier succeeded in defect remediation in a colloidal crystal [8], while the colloidal crystal was produced in a large area spontaneously by using micrometer-sized particles.

The present work demonstrates that the optical gradient force can reversibly control the assembly and the color of colloidal gold nanoparticles confined in the focal spot. We chose gold nanoparticles because their assemblies are reflected in the extinction spectrum. The extinction spectral measurements of trapped nanoparticles were successful by using a quasiconfocal system developed for the present study.

**II. EXPERIMENT**

The experimental setup is depicted in Fig. 1. A continuous wave of a  $Nd^{3+}$ :YAG (yttrium aluminum garnet) laser (Spectron, SI-903U; wavelength 1064 nm) was introduced into an optical microscope (Zeiss, UMSP50). This beam was focused into the colloidal gold via a microscope objective (magnification  $\times 100$ , numerical aperture 1.25). The spot shape was close to a Gaussian profile with 620 nm full width at half maximum in the focal plane. The colloidal gold was dropped on a depression in a slide glass and was sandwiched between the slide glass and a cover slip. Slightly collimated white light from a halogen lamp (Nippon P.I., PICL-NEX) was illuminated onto a sample from the opposite side of the objective. The transmission spectrum of the white light through the sample solution was measured by a polychromator (Oriel Instruments, 77480) with a charge-coupled device (CCD) camera (Andor, DU420-OE). A pinhole placed at the conjugate spot of the laser focus limited the detection area of the transmitted light to a spot 1  $\mu m$  in diameter centered on the focal point.

Colloidal gold suspended in water (BBInternational, EM.GC 40; mean diameter 40.5 nm,  $9 \times 10^{10}$  particles/ml) was used without further treatment. Extinction spectra of the

---

\*Author to whom correspondence should be addressed. FAX: +81-6-6879-7840.

Email address: yosikawa@ap.eng.osaka-u.ac.jp

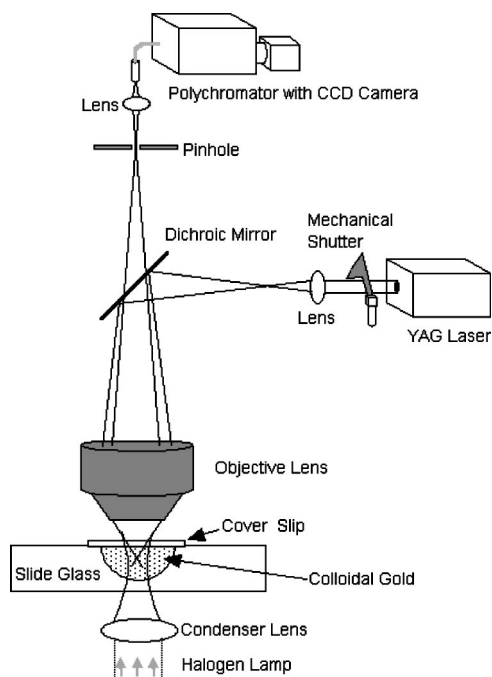


FIG. 1. A schematic diagram of the experimental setup to measure the extinction spectrum of the gold-nanoparticle assembly produced by optical trapping.

colloidal sample were measured by using a commercial visible absorption spectrometer (Shimadzu, UV-3100PC). They showed a single peak around 530 nm attributed to the surface plasmon resonance (SPR), and a broadening or an additional band indicating aggregation or polydispersion was not observed. This spectral feature proves a monodispersity of colloidal particles. The size distribution of the sample confirmed by means of dynamic light scattering (Otsuka Electronics, DLS-70SAr) had 7% standard deviation. The  $pH$  and the zeta potential of the sample were  $\sim 6.4$  and  $-39$  mV, obtained by a  $pH$  meter (Horiba, B-212) and a zeta potential analyzer (Malvern Instruments, Zetasizer Nano-ZS), respectively.

Extinction spectra of trapped gold nanoparticles were obtained as follows. First, the spectrum of the transmitted white light through the sample,  $I_b(\lambda)$ , was measured without laser irradiation. Next, the laser beam was irradiated by opening a mechanical shutter and another spectrum,  $I_t(\lambda)$ , was measured 10 s after the start of the laser irradiation. This 10 s is the waiting time for trapping of enough gold nanoparticles.  $I_t(\lambda)$  includes a little signal depression, because a part of the illumination light is absorbed by trapped nanoparticles which have emerged on the light path. By calculating  $[I_b(\lambda) - I_t(\lambda)]/I_b(\lambda)$ , the extinction spectra of the trapped nanoparticles were obtained.

### III. RESULTS AND DISCUSSION

Figure 2 shows the extinction spectra of the trapped gold nanoparticles. Each spectrum is measured for different laser powers [(a) 0, (b) 100, (c) 150, (d) 200, (e) 300, (f) 450, (g) 600, (h) 750, (i) 900 mW]. Since the gradient force exerted on a nanoparticle is proportional to the laser power, the number of trapped particles is reduced with decreasing laser power. Actually, the spectrum measured with 100 mW [Fig. 2(b)] of laser power is not clear as compared to other ones measured with higher laser powers, indicating that fewer nanoparticles are trapped. In the cases of 200 (c) and 300 mW (d) of laser power, a single extinction band corresponding to the SPR band is clearly observed. As laser intensity increases further, another extinction band around 700 nm appears and grows. Here it is an experimental artifact that the signal intensity goes down to 0 as the wavelength approaches 750 nm, because it reflects the specifications of the dichroic mirror equipped in the microscope. Therefore the second SPR band around 700 nm may have its actual peak in the longer wavelength region. However, it is a fact that the spectral shape, especially the intensity of the second SPR band in the longer wavelength region, is strongly dependent on the laser power.

Apart from the precise spectral shape, which could be determined theoretically if the inner structure of the nanoparticle

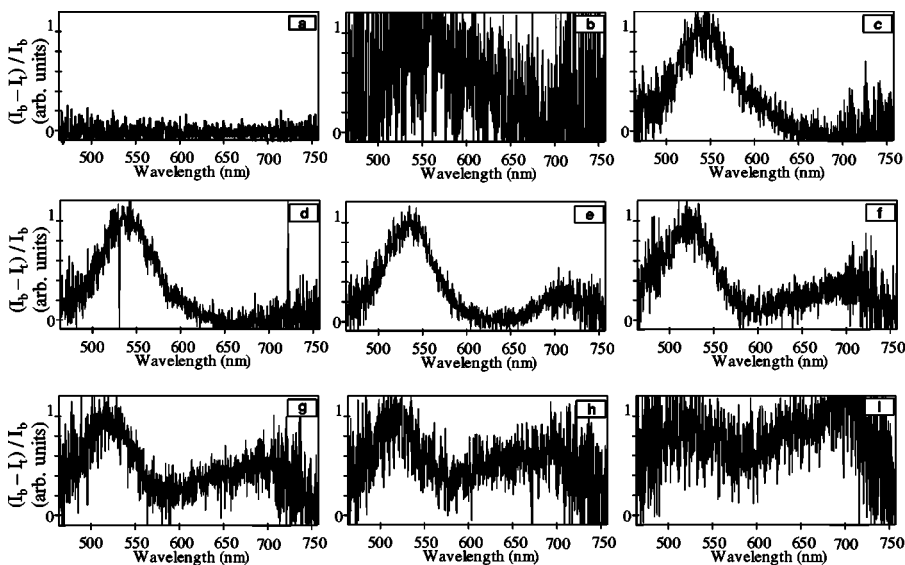


FIG. 2. Extinction spectra of trapped gold nanoparticles. All spectra measured at different laser powers [(b) 100, (c) 150, (d) 200, (e) 300, (f) 450, (g) 600, (h) 750, and (i) 900 mW] are normalized.

ticle assembly were known, the general aspect of the extinction spectral shape and its laser power dependence can be discussed. It was well known for a long time that such double peak extinction spectra were due to the aggregation of gold nanoparticles [9]. According to the generalized Mie theory, the second extinction band shown in the longer wavelength region is ascribed to the longitudinal SPR excitation for nonspherical or aggregated nanoparticles [10]. It should be noted that not only permanent aggregates, but also just assembled nanoparticles (located close to each other), show the second band because of collective electromagnetic oscillations between neighboring nanoparticles. The peak height, wavelength, and bandwidth of the first and second bands are strongly dependent on the disposition of nanoparticles and the interparticle distances in their assembly [11].

First, we consider and discuss the deformation of nanoparticles which may be induced by ablation and melting due to intense laser irradiation and could be responsible for the spectral change. Takami *et al.* reported the fragmentation of gold nanoparticles by irradiation with 532 nm nanosecond laser pulses in colloidal solution [12]. They observed a peak shift of the SPR band from 531.5 to 517 nm along with the laser irradiation according to the fragmentation of the gold nanoparticles. Link and El-Sayed investigated the deformation of gold nanoparticles induced by irradiation with a femtosecond pulse laser [13]. In their case, rod-shaped nanoparticles changed their conformation into a sphere shape; i.e., a change from the unstable to the stable shape was induced. Such deformation led to a spectral change from a double peak shape to a single peak one, since the rod-shaped gold nanoparticles show double peak extinction spectra in which the second band is ascribed to the longitudinal SPR. In these two works, the authors explained that photothermal heating induced by pulsed laser irradiation leads to the deformation of the gold nanoparticles. Since these spectral changes are totally different from our results, we can exclude the deformation and fragmentation of gold nanoparticles induced by such a photothermal process.

Another possibility is the aggregation of the colloidal gold promoted by laser irradiation. Eckstein and Kreibitz found that the formation of aggregates was accelerated by irradiation with visible laser beams (514 nm) [14]. They explained that the laser beam coupled with SPR caused additional attractive forces between particles via electromagnetic multipole interactions. Kimura and co-workers also reported photoinduced coagulation of gold nanoparticles suspended in 2-propanol [15,16]. In these past works, the crucial difference from our work is the wavelength and power of the laser. Their results were achieved by strong light absorption assigned to the SPR of gold nanoparticles, while we performed under off-resonance conditions by use of a 1064 nm cw laser. In our case, however, the laser power density ( $\sim$ MW/cm<sup>2</sup>) is higher than those in other works mentioned above. Therefore it is supposed that temperature elevation must take place due to laser absorption of gold nanoparticles and/or water, even if it does not reach the melting point. In particular in our case, as gold nanoparticles are gathered by a focused laser, the local concentration of nanoparticles increases in the focal spot. Such crowding of gold nanoparticles gives many chances to make irreversible aggregates. It

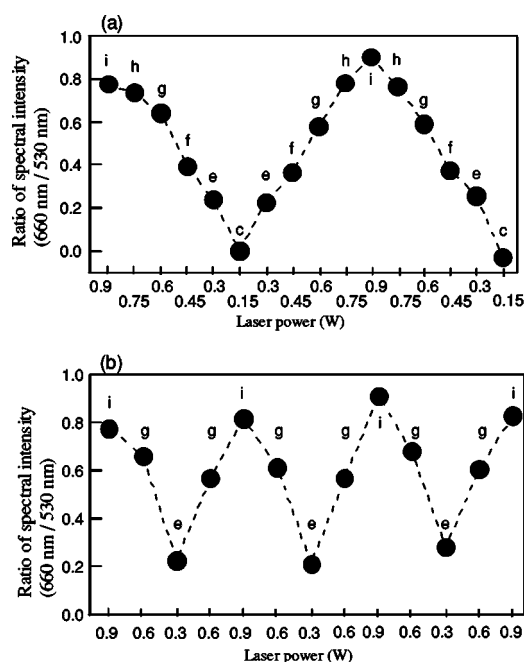


FIG. 3. Ratios of two bands ( $660\pm 5.6$  to  $530\pm 5.6$  nm) plotted as a function of laser power. Letters beside each data point correspond to laser powers used in Fig. 2 [i.e.; (c) 150, (e) 300, (f) 450, (g) 600, (h) 750, (i) 900 mW]. Since each data point is arranged in the order of measurement time, this indicates the change of the spectral shape by tuning of the laser power. The laser power was kept constant during a measurement of each spectrum (for 10 s), followed by the next measurement after a quick change of the power. (a) This procedure repeated 15 times between 150 and 900 mW in steps of 150 mW and (b) 12 times between 300 and 900 mW in steps of 300 mW.

is suspected that a combination of the concentration increase and temperature elevation could accelerate the formation of aggregates.

This suspicion about aggregation was excluded by confirming reversible changes of extinction spectra. Figure 3 shows the intensity ratios of two peaks plotted as a function of the laser power. This series of extinction spectra was measured without interruption of the laser irradiation, as follows. The first spectrum was measured after 10 s of laser irradiation. Without interruption of the laser irradiation, the laser intensity was changed quickly to the next power, and immediately a second spectrum was measured with the same integration time. These procedures were repeated a few times for three [Fig. 3(a)] and six [Fig. 3(b)] laser powers corresponding to (c)–(i) in Fig. 2. Each spectrum was measured every 17 s and the integration time for each measurement was 10 s. The spectral intensity ratio between the second band and the first one ( $660$  to  $530$  nm) is estimated for each spectrum and plotted in order of the measurement. Figure 3 shows that the spectral shape follows the laser power reversibly and repeatedly.

Here we summarize the potential energy and shapes in the present experiment for the sake of later discussion. Since the gradient force is dominant for optical trapping of a 40 nm sized gold nanoparticle as proved by Svoboda and Block [17], its potential  $U$  can be expressed by the following equation:

$$U \cong -\frac{|\alpha||E|^2}{2} = -\frac{I}{c} 3V \left| \frac{(n/n')^2 - 1}{(n/n')^2 + 2} \right|. \quad (1)$$

Here  $c$  is the velocity of light in vacuum,  $n$  and  $n'$  are the refractive indices of gold and the surrounding medium (water), and  $V$  is the volume of a gold nanoparticle.  $I$  is the laser intensity (power per unit area,  $\text{W}/\text{m}^2$ ) with a Gaussian beam profile, and described in the focal plane as

$$I(r) \cong \frac{P}{2\pi r_0^2} \exp\left(-\frac{r^2}{2r_0^2}\right), \quad (2)$$

where  $r$  is the distance from the center of the focal spot and  $P$  is the laser power.  $r_0$  was estimated as 440 nm from the beam profile measurement. The polarizability  $\alpha$  is estimated approximately according to the calculation used in [17]. Substituting Eq. (2) into Eq. (1), the potential energy  $U$  is represented as

$$U(r) \cong U_0 \exp\left(-\frac{r^2}{2r_0^2}\right), \quad (3)$$

where  $U_0$  is calculated as  $\sim -6.2kT$  ( $k$  is the Boltzmann constant and  $T$  is temperature,  $kT = 4.12 \times 10^{-12}$  J) at 100 mW of laser power and is proportional to the laser power (i.e.,  $-9.3kT$  at 150 mW,  $-12.4kT$  at 200 mW, and so on).

Trapped materials escape from the focal spot with a certain probability that is determined by the depth and shape of the trapping potential. Therefore if gold nanoparticles come in and escape from the focal spot during spectral measurements, the obtained extinction spectra (Figs. 2 and 3) can be ascribed to many different nanoparticles. As described in some papers [17,18], the escape time, which is defined by the time during which one particle stays in the potential well, can be calculated as  $\sim 0.46$  s in the case of 100 mW of laser power ( $U_0 \sim -6.2kT$ ) and  $\sim 6.8$  s in the case of 150 mW ( $-9.3kT$ ), and it increases exponentially with increasing laser power. Actually, we confirmed that the same extinction spectra were observed over a 1 min period or longer, as long as the laser beam irradiated continuously with the same power. Therefore it is supposed that gold nanoparticles once captured in the focal spot can hardly escape during the series of spectral measurement in Fig. 3. When the laser power is changed during optical trapping, if irreversible aggregates were formed, the second extinction band would not be reduced with a decrease of the laser power, because aggregates once formed cannot be dispersed into single nanoparticles again. That is, Fig. 3 demonstrates that trapped nanoparticles were separate from each other without making permanent aggregates and they were just gathered at the focal point by the gradient force. This spectral change also indicates the order of interparticle distances, because the coupling of surface plasmon modes between two gold nanoparticles is effective only below the order of some tens of nanometers [19,20].

The size, shape, and inner structure of the assembly are determined by the trapping potential and interparticle interactions. The depth of the potential energy produced by the focused laser beam was estimated as  $\sim 6.2kT$  (at 100 mW of laser power) to  $\sim 56kT$  (at 900 mW) as mentioned above. At

the beginning of the discussion about the inner structure, the number of trapped nanoparticles is roughly estimated from the optical density of a SPR peak in the extinction spectrum under the assumption of the Beer-Lambert law. The extinction cross section of a single gold nanoparticle used in the present study was  $2.3 \times 10^3 \text{ nm}^2$  at the SPR peak wavelength. On the other hand, the optical density of the assembly trapped in the focal spot was estimated as  $\sim 0.045$  from Fig. 2(e). Under the assumption that the assembly was confined in a spot 1  $\mu\text{m}$  in diameter, the number of nanoparticles involved in the assembly was estimated as  $\sim 35$ . A similar particle number is obtained from another estimation which is based on the trapping rate measured by the single particle counting method [21]. As the effective trapping region is roughly defined as the beam width at which the potential depth has decreased to  $kT$ , the width of the trapping region is estimated as  $\sim 1 \mu\text{m}$  in the axial and  $\sim 3 \mu\text{m}$  in the radial directions at 100 mW of laser power. This means that the volume of the trapping region is much larger than that of the assembly ( $\sim 35$  nanoparticles) trapped in it and the number of trapped nanoparticles should increase with increasing laser power because there is space to accept another nanoparticle. However, the signal intensity of the extinction spectra appears to decrease at high laser power as shown in Figs. 2(g)–2(i). This is reasonable because, if such scattering matter as gold nanoparticles fills the trapping potential, they strongly disturb the focused laser beam and cannot be sustained by such a disturbed laser spot. Based on these considerations, we have deduced that the number of trapped gold nanoparticles is not high enough to fill the focal spot even in the case of high laser power, and the nanoparticles are confined in almost the bottom region of the trapping potential.

Colloidal gold suspended in water is stabilized by the electrostatic force. Negative charges created by surface-stabilizing ions form an electric double layer around the particle surface. The repulsive potential produced by this double layer and the attractive potential caused by van der Waals interaction determine the total interaction between colloidal particles. Generally this total potential (so-called Derjaguin-Landau-Verwey-Overbeek potential) works as a repulsive interaction when the interparticle distance (surface to surface) is over a few nanometers, and decreases exponentially within the order of tens of nanometers, and this potential barrier is comparable to the energy of the thermal motion  $kT$  [14,22].

Let us consider the situation that gold nanoparticles dressed in electrostatic potential barriers are confined in an optical microcage produced by a focused laser beam. Figure 4 shows a schematic image of the colloidal assembly formed by optical trapping. Nanoparticles are gathered in the center of the focal spot, i.e., the bottom of the trapping potential as mentioned above, but are separated from each other by electric double layers. It is noteworthy that the potential depth around trapped nanoparticles is comparable to and can be controlled by the order of the interparticle repulsive interaction. If the potential depth of the optical trapping were much larger than the interparticle interactions, nanoparticles would be packed tightly into the focal spot without any space to change their locations. The soft confinement is a key point to realize reversible control of colloidal assemblies.

Furthermore, the extinction spectral shape gives information about the morphology of the assembly also. The relation

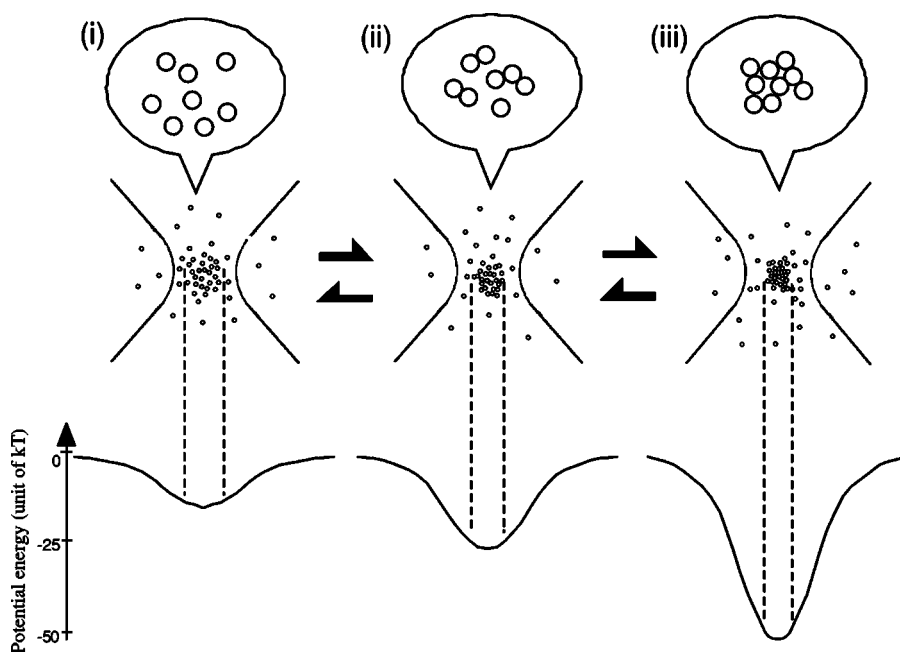


FIG. 4. Top and middle: Schematic image of reversible conformational changes of the trapped gold-nanoparticle assembly. Expanded images of the assembly are illustrated in balloon. Bottom: Profiles of potential produced by the focused laser beam. (i) Nanoparticles prefer to stay in the focal spot because the potential depth is larger than the energy of Brownian motion. Nanoparticles are separated from each other, so that an extinction spectrum ascribed to isolated gold-nanoparticles is obtained, as shown in Figs. 2(b)–2(d). (ii) As laser power becomes higher, nanoparticles start to approach each other and make small assemblies like doublets or triplets. Assemblies take a kind of one-dimensional conformation because repulsive interactions between nanoparticles prevent compact morphologies, presenting double peak spectra like Figs. 2(e) and 2(f). (iii) Higher laser power produces more compact assemblies consisting of various numbers of nanoparticles and morphologies, resulting in broader spectra with large components in the longer wavelength region, as shown in Figs. 2(h) and 2(i).

between morphology and optical properties of aggregates was studied theoretically and experimentally in the past work [10]. In the case of fast aggregation (e.g., aggregation induced by addition of electrolytes), compact three-dimensional aggregates with various sizes are formed and they show broad SPR spectra rather than distinct peaks because of inhomogeneous broadening [10]. On the other hand, slow aggregation of stabilized colloids prefers to produce one-dimensional structures. In this case, after a nanoparticle bonds with another one, a third one can hardly approach the connecting point of the doublet due to the strong repulsive potential of the electric double layers, resulting in a connection to the head or tail of the doublet and leading to the formation of linearlike structures [23]. Generally such one-dimensional aggregates show a distinct double peak feature in the extinction spectrum that is similar to our results shown in Fig. 2. In our case, since gold nanoparticles wearing electric double layers are confined in a microcage of optical trapping, they are forced to make assemblies and take one-dimensional structures against the repulsive forces.

In addition to the self-assembly, another mechanism can be considered as a cause to make gold nanoparticles close to and aligned with each other in the optical microcage. It is the so-called optical binding effect, which has been proposed and demonstrated by some research groups [24–26]. This effect is considered as a dipole-dipole interaction induced by the strong electromagnetic field of the laser beam. The dipole moment of trapped gold nanoparticles induced by the fo-

cused laser beam would produce an attractive force and make a linearlike structure that aligns in parallel with the laser polarization. Since this force is effective at short distance and evanescent in far field, optical trapping to confine nanoparticles densely is indispensable for it. Furthermore, the trapping potential is modulated by trapped gold nanoparticles because of the scattering of the light. Therefore, strictly described, nanoparticles are trapped in the sum of incident and scattered electromagnetic fields produced by themselves. It is very difficult to solve such a self-consistent field and further investigation is needed to identify the assembling structure and mechanism.

#### IV. CONCLUSION

We have demonstrated that optical trapping can control the assembly of gold nanoparticles reversibly. An extinction band ascribed to SPR of assembled nanoparticles appeared and grew with increase of laser intensity due to conformational change of the gold-nanoparticle assembly. The feature of the assembly in the focal spot was discussed on the basis of spectral shape, trapping potential, and interparticle interactions. This work shows that the optical microcage must be useful for the microassembly formation of various colloidal particles stabilized by the electrostatic force. In particular,

SPR sensors using gold nanoparticles [27,28] would be a promising target, since a slight change of the assembly induced by surface adsorption of objective molecules is strongly reflected in the extinction spectrum. In addition, by combining with a fixation technique for trapped nanoparticles [4], optical trapping will develop into an integrated technique for nanomaterials.

#### ACKNOWLEDGMENTS

This research was partly supported by a Grant-in-Aid for Scientific Research (KAKENHI)(S) (14103006) from the Japan Society for the Promotion of Science and a Grant-in-Aid for Young Scientists (B) (14740384) from the Ministry of Education, Culture, Sports, Science and Technology.

- 
- [1] J. Hotta, K. Sasaki, and H. Masuhara, *J. Am. Chem. Soc.* **118**, 11968 (1996).
- [2] J. Hofkens, J. Hotta, K. Sasaki, H. Masuhara, T. Taniguchi, and T. Miyashita, *J. Am. Chem. Soc.* **119**, 2741 (1997).
- [3] S. Masuo, H. Yoshikawa, T. Asahi, and H. Masuhara, *J. Phys. Chem. B* **106**, 905 (2002).
- [4] S. Ito, H. Yoshikawa, and H. Masuhara, *Appl. Phys. Lett.* **78**, 2566 (2001); **80**, 482 (2002).
- [5] A. Ashkin, *Phys. Rev. Lett.* **40**, 729 (1978).
- [6] A. Ashkin, J. M. Dziedzic, J. E. Bjorkholm, and S. Chu, *Opt. Lett.* **11**, 288 (1986).
- [7] P. P. Jose and B. Bagchi, *J. Chem. Phys.* **116**, 2556 (2002).
- [8] P. T. Korda and D. G. Grier, *J. Chem. Phys.* **114**, 7570 (2001).
- [9] J. Turkevich, G. Garton, and P. C. Stevenson, *J. Colloid Sci.* **9**, 26 (1954).
- [10] U. Kreibig, *Z. Phys. D: At., Mol. Clusters* **3**, 239 (1986).
- [11] U. Kreibig and M. Vollmer, *Optical Properties of Metal Clusters* (Springer-Verlag, Berlin, 1994).
- [12] A. Takami, H. Kurita, and S. Koda, *J. Phys. Chem. B* **103**, 1226 (1999).
- [13] S. Link and M. A. El-Sayed, *J. Phys. Chem. B* **103**, 8410 (1999).
- [14] H. Eckstein and U. Kreibig, *Z. Phys. D: At., Mol. Clusters* **26**, 239 (1993).
- [15] N. Satoh, H. Hasegawa, K. Tsujii, and K. Kimura, *J. Chem. Phys.* **98**, 2143 (1994).
- [16] Y. Takeuchi, T. Ida, and K. Kimura, *J. Phys. Chem. B* **101**, 1322 (1997).
- [17] K. Svoboda and S. M. Block, *Opt. Lett.* **19**, 930 (1994).
- [18] A. Simon and A. Libchaber, *Phys. Rev. Lett.* **68**, 3375 (1992).
- [19] S. A. Maier, P. G. Kik, and H. A. Atwater, *Appl. Phys. Lett.* **81**, 1714 (2002).
- [20] S. A. Maier, M. L. Brongersma, P. G. Kik, and H. A. Atwater, *Phys. Rev. B* **65**, 193408 (2002).
- [21] C. Hosokawa, H. Yoshikawa, and H. Masuhara, *Phys. Rev. E* (to be published).
- [22] J. N. Israelachvili, *Intermolecular and Surface Forces* (Academic, London, 1992).
- [23] B. V. Enustun and J. Turkevich, *J. Am. Chem. Soc.* **85**, 3317 (1963).
- [24] M. M. Burns, J. M. Fournier, and J. A. Golovchenko, *Phys. Rev. Lett.* **63**, 1233 (1989).
- [25] P. C. Chaumet and M. Nieto-Vesperinas, *Phys. Rev. B* **64**, 035422 (2001).
- [26] F. Depasse and J.-M. Vigoureux, *J. Phys. D* **27**, 914 (1994).
- [27] T. Okamoto, I. Yamaguchi, and T. Kobayashi, *Opt. Lett.* **25**, 372 (2000).
- [28] N. Nath and A. Chilkoti, *Anal. Chem.* **74**, 504 (2002).